Preparation and Properties of Poly(imide siloxane) Segmented Copolymer/Silica Hybrid Nanocomposites

Wen-Chang Liaw,[1] Kuan-Pin Chen[2]

[1]*Department of Chemical Engineering, Nation Yunlin University of Science and Technology, Touliu, Yunlin 640, Taiwan, Republic of China*
[2]*Graduate School of Engineering Science and Technology (Doctoral Program), Nation Yunlin University of Science and Technology, Touliu, Yunlin 640, Taiwan, Republic of China*

Received 3 August 2006; accepted 30 January 2007
DOI 10.1002/app.26319
Published online 2 April 2007 in Wiley InterScience (www.interscience.wiley.com).

ABSTRACT: A series of Poly(imide siloxane) (PIS)/silica (SiO_2) hybrid nanocomposites with C-Si covalent bonding between the homogeneous PIS copolymer and SiO_2 have been successfully synthesized. The PIS copolymer synthesized in this study is characterized by the coexistence of two segments: the polyimide segment and polydimethyldiphenylsiloxane segment, and the latter are specially featured with the introduction of a diphenyl group for improved homogeneity. The PIS/SiO_2 hybrid nanocomposites were prepared from 3,3′,4,4′-bezonphenone tetracarboxylic dianhydride (BTDA), 2-2′-bis[4(3-aminophenoxy)-phenyl] sulfone (*m*-BAPS), and vinyl-containing α,ω-bis-(aminopropyl)polydimethyldiphenyl siloxane (APPPVS) oligomer to form vinyl siloxane-containing poly(amic acid) (PAAVS). This copolymer was further reacted with trimethoxyvinylsilane (TMVS), 2,2′-azobis-isobutyronitrile (AIBN), and tetraethoxysilane (TEOS). The PIS/SiO_2 hybrid nanocomposites exhibited a series of properties unlike traditional composites, and the nano sized inorganic particles have resulted in a transparent hybrid when the SiO_2 content was less than 12 wt %. The Young's modulus and tensile strength of the PIS/SiO_2 hybrid nanocomposites increased with increasing SiO_2 content, whereas, the elongation at break was only slightly affected. The structure of the hybrids was characterized by FTIR, ^{29}Si-NMR, ^{1}H-NMR, and ^{13}C-NMR, as well as SEM and TEM. The thermal properties of the PIS/SiO_2 hybrid nanocomposites were investigated with DSC, TGA, and DMA studies. © 2007 Wiley Periodicals, Inc. J Appl Polym Sci 105: 809–820, 2007

Key words: polyimide; polysiloxane; silica; microstructure; nanocomposites

INTRODUCTION

Polyimide (PI) is a family of high-performance polymer materials characterized by excellent thermal stability, superior mechanical, and electrical properties which have wide applications in the aerospace and microelectronic industries.[1–6] Organic–inorganic hybrid nanocomposites have become an attractive source for advanced materials as they usually exhibit unique properties that lack of conventional materials.[7–14] The incorporation of nanosized inorganic particles such as SiO_2 is considered to be an effective means in the synthesis of nanocomposites.

Phase separation commonly happens in organic–inorganic hybrid nanocomposites systems. Observable phase separation tends to develop at certain size of inorganic nano particle, which in turn, is usually related to the overall inorganic content. High inorganic content is likely to promote particle size increase, and results in a composite that is opaque. However, by minimizing the size of the inorganic domain, phase separation might be kept below an acceptable level so that the transparency of the material would not be affected. It has been demonstrated in earlier studies that the production of a transparent PI/SiO_2 hybrids nanocomposites was limited to the condition in which the SiO_2 content was less than 10 wt %.[15,16]

These organic–inorganic hybrid nanocomposites can be synthesized by *in situ* sol-gel reaction which consists of two steps in the formation of nanoparticals: (1) the hydrolysis of metal alkoxides to produce metal hydroxide and (2) the formation of a three-dimensional network of metal oxide by polycondensation.

The introduction of chemical bonds between organic and inorganic molecules would bring about the effect that the barrier between these two phases was macroscopically blurred by such chemical modification, which improved the optical, as well as other desirable properties.

Recently, several kinds of PI with terminal alkoxy silanyl groups have been developed and were utilized for the design of new categories of organic–inorganic hybrid materials.[17–24]

Correspondence to: W.-C. Liaw (liawwc@yuntech.edu.tw).
Contract grant sponsor: National Science Council; contract grant number: NSC 92-2216-E-224-002.

Many researchers[25–28] in their separate studies, prepared PI/SiO_2 hybrid nanocomposites with the amino group substituted alkoxysilane, for example, aminophenyltrimethoxysilane (APTMOS), aminopropyltriethoxysilane, aminopropylmethyldiethoxysilane, and diaminopropyltetramethyl disiloxane. They found that both the amino and alkoxy groups on these silanes provided chances of chemical bond formations between the organic PI polymer and inorganic SiO_2 networks, which led to a more homogeneous and transparent PI/SiO_2 hybrid nanocomposite films as compared to those prepared using only PI and tetraexthoxysilane (TEOS). The former hybrid nanocomposites, in general, showed better mechanical properties. The modulus and ultimate strengths increased and the elongation at break decreased with increasing SiO_2 content.

Shang and Zhu[29] made PI/SiO_2 nanocomposites by hybridizing BTDA and 4-4′-diamino-3-3′-dimethyldiphenylmethane (MMDA), γ-glycidyloxypropyl trimethoxysilane (GPTMOS), and TEOS. These hybrids were reported to improve the compatibility between PI and SiO_2 and, at the same time, improved the mechanical properties, thermal properties, and optical properties.

Chen and Chiu[30] produced soluble PI from 4,4′-diamino-4′-hydroxytriphenyl-methane (DHTM) and pyromellitic dianhydride (PMDA). The synthesized soluble PI was then dissolved in NMP, followed by reaction with GPTMOS and TEOS to form PI/SiO_2 hybrid nanocomposite thin film. When the SiO_2 content is less than 15 wt %, the diameters of silica particles were less than 100 nm, which is well-dispersed throughout the composite matrix. Enhanced thermal stability and mechanical properties were attained.

The polysiloxane has been known to interact with SiO_2 closely because of the similarity of its structure (—Si—O—Si—) with the sol-gel glass matrix of the SiO_2 precursor,[31] which indicated that a copolymer of PI and polysiloxane, poly(imide siloxane) (PIS), might be a good candidate material for organic–inorganic hybrid nanocomposites. However, to date, few reports about the synthesis and properties of PIS/SiO_2 hybrid nanocomposites could be found.[26,32]

Park and Kim[32] prepared a series of siloxane-containing poly(amic acid) (PAAS) from amine-terminated polydimethylsiloxane (PDMS, $M_n = 900$ g mol^{-1}), 4-4′-oxydianiline (ODA), pyromellitic dianhydride (PMDA), and aminopropyltriethoxysilane (APrTEOS). Then, TEOS were added to the PAAS solution and followed by imidization to form the PIS/SiO_2 hybrid nanocomposite. The results showed that the introduction of PDMS into a PI matrix retarded the phase separation of hybrid composites. Meanwhile, the formation of high-molecular-weight SiO_2 was prevented.

In this study, we intent to synthesize PIS/SiO_2 hybrid nanocomposites by means of providing chemical bond formations between the inorganic SiO_2 network and the organic sloxane segment (of vinyl group containing PIS copolymer), through the introduction of a coupling agent (trimethoxyvinylsilane, TMVS). It was anticipated that this would improve the thermal and mechanical properties of the material.

Because of the large solubility parameter difference between PI and PDMS, there exist interfacial gap between the two segments. Consequently, such gap may lead to microphase separation. To minimize the interfacial gap, we introduced diphenylsiloxane into the PDMS segment. The proposed strategy involves the design of randomly arranged flexible polydimethyldiphenylsiloxane segments, and incorporation of this segment at random positions of the PI backbone.

EXPERIMENTAL

Materials

1,3-bis(3-aminopropyl)1,1,3,3-tetramethyldisiloxane (DSX, purity > 97%); octamethyl-cyclotetrasiloxane (D_4, purity > 97%); octaphenylcyclotetrasiloxane (P_4, purity > 98%) were obtained from Fluka. Tetramethyltetravinylcyclotetrasiloxane (V_4, purity > 98%) and TMVS were purchased from Shin-Etsu Chemical. 3,3′,4,4′-bezonphenone tetracarboxylic dianhydride (BTDA) was purchased from Aldrich, which was purified by recrystallization from a high-purity acetic anhydride, followed by vacuum drying at 120°C for 14 h. 2-2′-bis[4-(3-aminophenoxy)phenyl]-sulfone (*m*-BAPS) was purchased from Lancast Synthesis. *N*-methyl-2-pyrrolidone (NMP) was purchased from Tedia, which was dried with 4 Å molecular sieves. Tetraethoxysilane (TEOS) was purchased from Aldrich. 2, 2′-azobis-isobutyronitrile (AIBN) was purchased from Showa Chemical.

Preparation of vinyl-containing α,ω-bis(aminopropyl)polydimethyldiphenyl siloxane

The synthesizing steps are shown in Scheme I. The vinyl-containing α,ω-bis(aminopropyl)polydimethyldiphenyl siloxane (APPPVS) was synthesized by anionic equilibrium polymerization. Basic phosphorous salt was used as the catalyst, while, D_4 (1.5 g), P_4 (2.5 g), and V_4 (2.5 g) were the comonomers and DSX served as the terminating agent.

The reaction conditions were described as follows. The reactants were first heated together to 120°C, to form a homogeneous reaction mixture, which was then cooled to 80°C, and held at this temperature for 48 h. The mixture was then heated to 150°C for 5 h to decompose the catalyst. After cooling to 110°C, the reactor was maintained at vacuum (∼ 0.1 Torr)

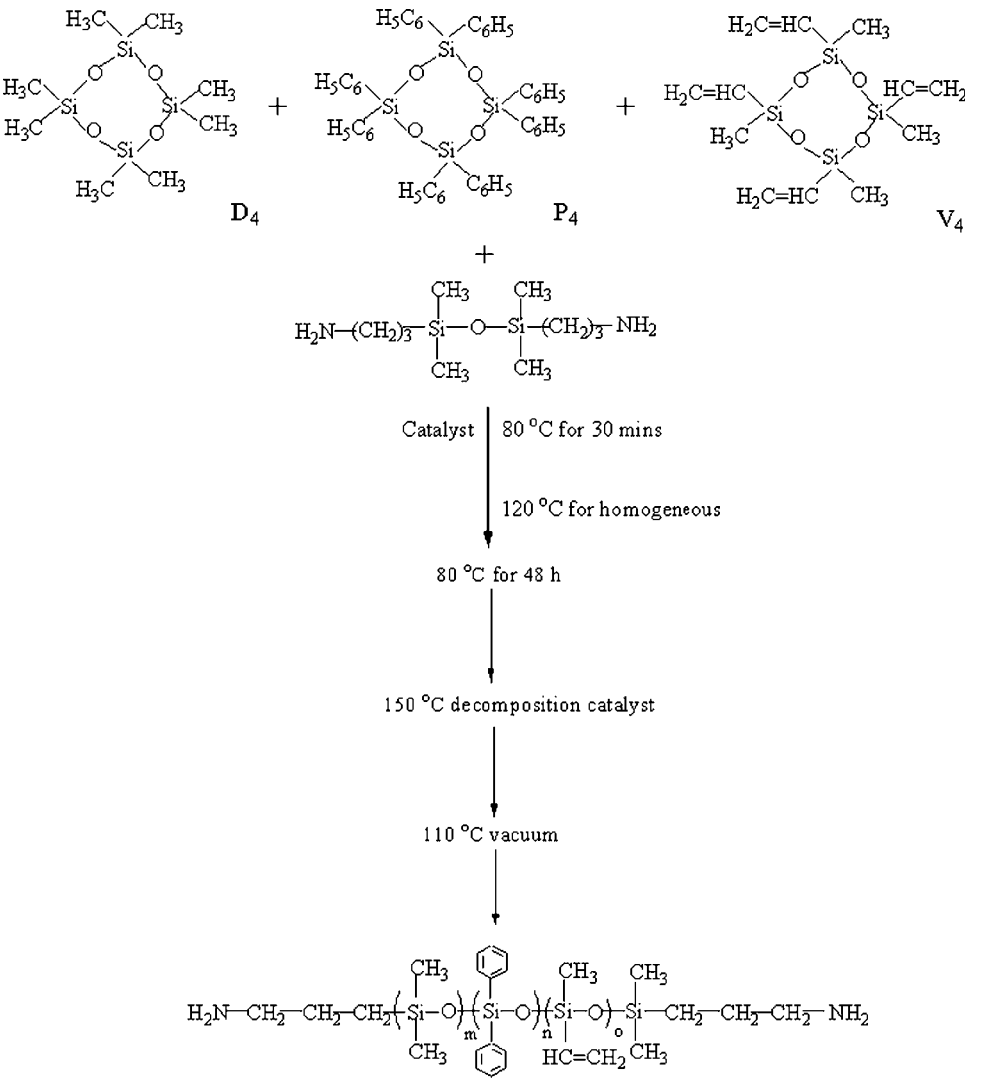

Scheme 1 Procedure for the synthesis of APPPVS.

for 4 h to remove unreacted monomers. The number–average molecular weight (M_n) was determined by gel permeation chromatography (GPC) and nuclear magnetic resonance (^{1}H-NMR) spectroscopy, and M_n was found to be 850 g mol^{-1}.

Preparation of vinyl siloxane-containing poly(amic acid)

The vinyl siloxane-containing poly(amic acid) (PAAVS) were prepared from BTDA, *m*-BAPS, and APPPVS (M_n = 850 g mol^{-1}, from Scheme I). The reactions steps are shown as in Scheme II.

In a typical reaction, *m*-BAPS (0.6091 g, 1.41 $\times$ 10^{-3} mol) and APPPVS (M_n = 850 g mol^{-1}) (0.0171 g, 2.0 $\times$ 10^{-5} mol) were dissolved in NMP with stirring. After complete dissolution, 0.4607 g of BTDA (1.42 $\times$ 10^{-3} mol) was then added. The mixture was stirred at room temperature for 12 h and a viscous PAAVS solution was obtained. The solid contents (w/w) is 25 wt %.

Preparation of PIS/SiO_2 hybrid nanocomposites

For the preparation of PIS/SiO_2 hybrid nanocomposites, equal normality of vinyl TMVS and PAAVS with 0.1 wt % AIBN diluted in NMP, were mixed and stirred at room temperature for 1 h. Then, a different mixture of TEOS with distilled water (1/4 mol of TEOS) and NMP as solvent were added (see Table I) to the above solution. The solution soon became homogenous, and was continuously stirred at room temperature for 6 h. The PIS/SiO_2 hybrid nanocomposites were prepared by casting the solution onto the PET sheet, followed by heating at 70–80°C for 2 h. The half-dried film was then peeled off the PET sheet, and transferred to another substrates and stepwise heat treated at 100, 150, 200,

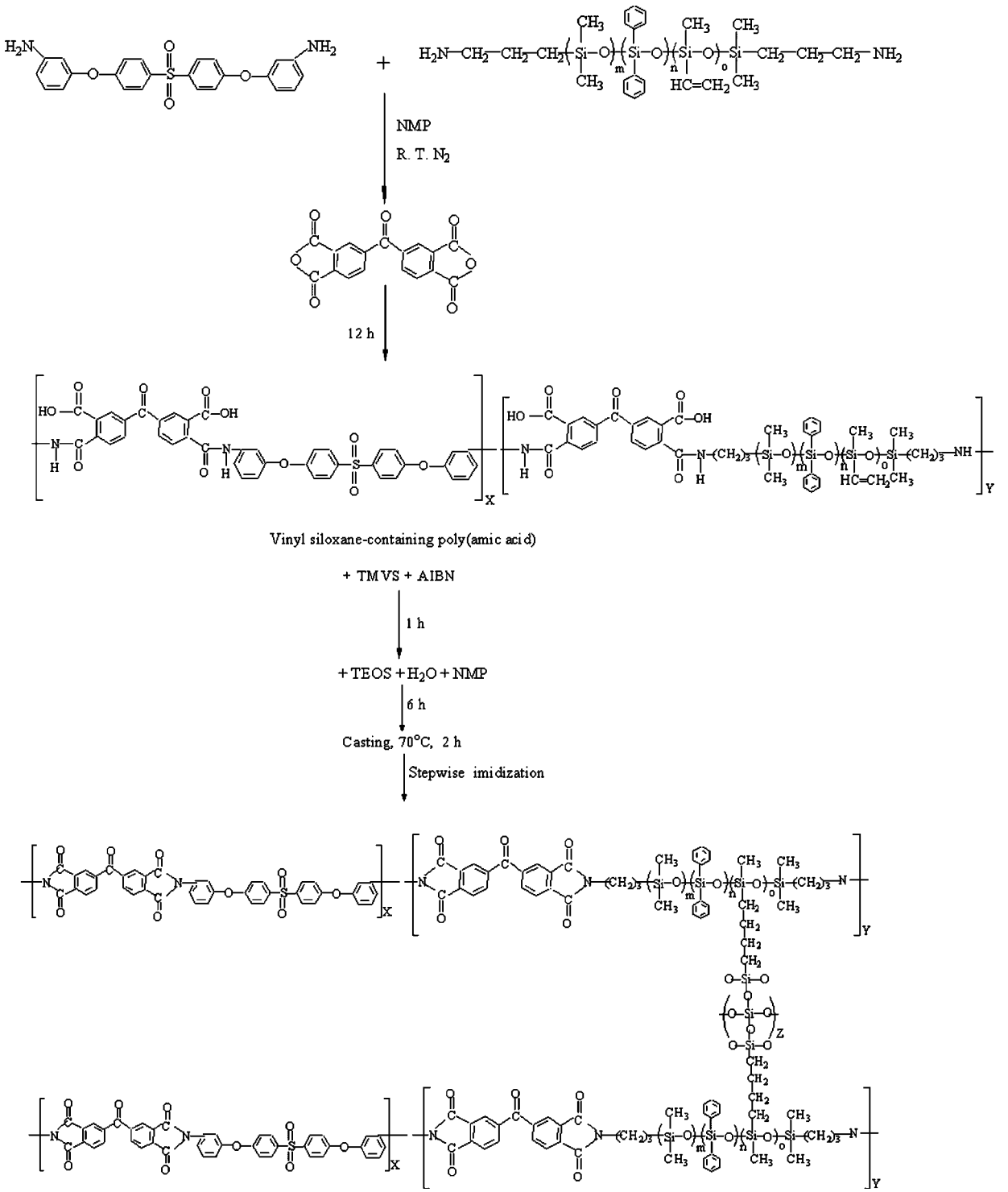

Scheme 2 Procedure for the synthesis of the PIS/SiO_2 hybrid nanocomposites.

250, and 300°C for each 1 h. The preparation was shown in Scheme II.

Measurements

The chemical structure were determined by ^{1}H-NMR spectra on bruker DPX-300 FT-NMR spectrometer at 500 MHz, ^{13}C- and ^{29}Si-NMR spectra were also measured at room temperature on the same spectrometer operating at 100 and 80 MHz. Infrared spectra of PAAVS and PIS/SiO_2 hybrid nanocomposites were determined on a Bruker ISF112V FTIR spectrophotometer. Glass transition temperature (T_g) was measured on a DuPont DSC 1090 instrument at a heating

TABLE I
Preparation and Opacity of the PIS/SiO_2 Hybrid Nanocomposites

Sample name	TEOS (g)	H_2O (g)	Silica content (wt %)		Opacity[b]
			Theory[c]	Experiment[d]	
PIS[a]	0	0	0	0	T
PIS/SiO_2-1	0.04	0.01	1	0.8	T
PIS/SiO_2-3	0.11	0.04	3	2.8	T
PIS/SiO_2-5	0.19	0.07	5	4.9	T
PIS/SiO_2-7	0.27	0.09	7	6.7	T
PIS/SiO_2-10	0.38	0.14	10	9.4	T
PIS/SiO_2-12	0.45	0.16	12	11.7	O
PIS/SiO_2-15	0.57	0.21	15	14.4	O
PIS/SiO_2-20	0.75	0.26	20	19.4	O
PIS/SiO_2-25	0.94	0.32	25	23.8	O
PIS/SiO_2-30	1.12	0.39	30	26.0	O

[a] All PIS was prepared with 1.4 wt % of vinyl-containing (*-bis(aminopropyl) polydimethyldiphenyl siloxane (APPPVS) and the same vinyl normality of TMVS.
[b] T, transparent; O, opaque.
[c] The theoretical silica content was calculated under the assumption that the sol-gel reaction proceeds completely.
[d] The experimental silica content was obtained from residual ash after heat treatment at 900°C in N2.

rate of 10°C min^{-1}. Thermal gravimetric analysis (TGA) measurements were performed on a Perkin-Elmer TGA in N_2 at a heating rate of 20°C min^{-1} from 25 to 900°C. The stress/strain curve was obtained from a DMA 2980 with control force mode. SEM images of the cross section of hybrid nanocomposites were taken on Jeol Model JSF 6700F field emission scanning electron microscope with inclusion of energy-dispersion X-ray analysis (EDS). Transmission electron microscope (TEM) with a JEOL-200 FX operating at 300 KV. X-ray diffraction (XRD) was measured with Bruker P4 single crystal X-ray diffractometer.

RESULTS AND DISCUSSION

The following scheme was proposed and conducted. We first synthesized the random copolymer, the APPPVS, which was used as the flexible segments in the PIS copolymers.

The randomly positioned diphenyl siloxane in APPPVS oligomer was expected to contribute in the increase of the compatibility between PI and polysiloxane segments in the PIS copolymer.

The above random copolymer was further copolymerized with BTDA and *m*-BAPS to form the PAAVS solution. The obtained copolymer solution was then added with TMVS, TEOS, and AIBN. The ratio between TEOS and PAAVS was adjusted, to study the effect of SiO_2 content on optical, thermal, and mechanical properties. When the free-radical reaction was initiated, sol-gel reaction, and thermal imidization took places as well. It is expected that the TMVS molecules will provide an opportunity of covalent bond formation between the inorganic SiO_2 and the PIS matrix.

Characterization

The newly synthesized organic–inorganic hybrid nanocomposites were first characterized spectrally by studying the FTIR, NMR, XRD, and EDS spectra. Its microstructure, as well as thermal and mechanical properties were also investigated and reported in the following sections.

FTIR analysis

To verify the conversion of PAAVS to PIS/SiO_2 hybrid nanocomposites, and to confirm the development of the SiO_2 formed within the imidized PIS, FTIR was used for the investigation. Figure 1 compared the FTIR spectra of the unimidized PAAVS to that of the imidized PIS/SiO_2-20 hybrid nanocomposite (SiO_2 content was 20 wt %).The FTIR spectra of PAAVS was characterized by broad absorption peak at 3000–3500 cm^{-1} because of the presence of OH-groups, while the amide group was responsible for the absorption peak at 1650 and 1541 cm^{-1}. The thermal imidization of PAAVS was evidenced by the disappearance of the absorption peak at 1650 and 1541 cm^{-1}, as well as 3000–3500 cm^{-1}. Meanwhile, the absorption peaks at 1780, 1720, 1380, and 725 cm^{-1} confirmed the formation of PIS copolymers.

The formation of the SiO_2 network, within the PIS matrix, changed the absorption pattern of the FTIR spectra, as reflected by the broadening of the absorp-

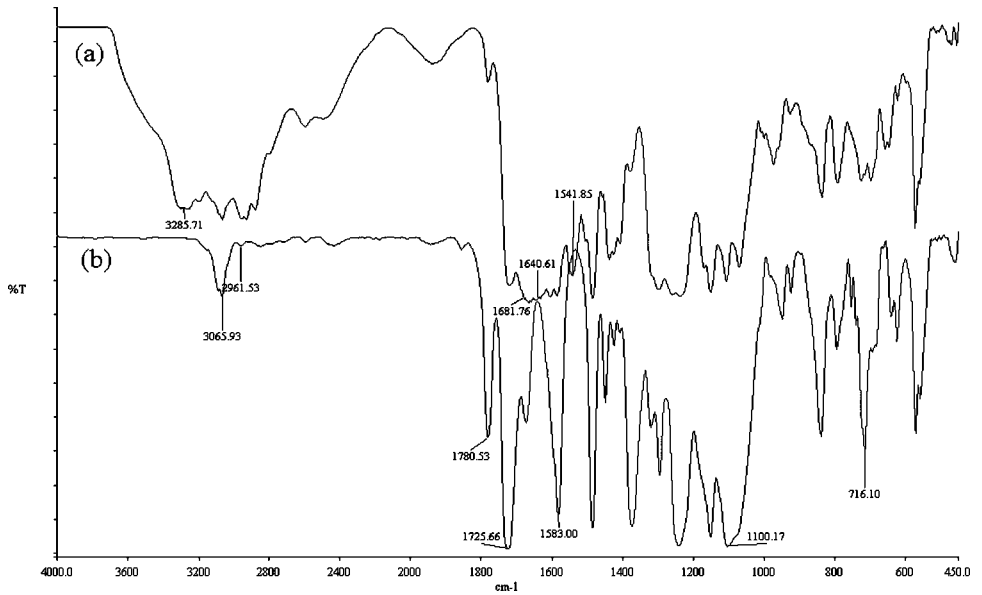

Figure 1 FTIR spectra of (a) PAAVS (b) PIS/SiO_2-20.

tion peak at 1000–1100 cm^{-1}, upon the increase of SiO_2 content (Fig. 2). This observation supports the aforementioned speculation that a three-dimensional Si—O—Si network has formed in the hybrid films.[33–35] On the other hand, the presence of dimethylsiloxane (Si-$(CH_3)_2$) blocks was evidenced by the C—H absorption at 2960 cm^{-1}. The presence of the dimethylsiloxane blocks is supposed to be beneficial, in terms of better processibility and modulation of the stiffness of the copolymer. In this study, besides dimethylsiloxane, diphenylsiloxane was copolymerized into the hybridized matrix, hoping that this would offer better compatibility between PI and polysiloxane blocks, while reducing the likelihood of phase separation. However, the absorption peaks of the phenyl groups on diphenylsiloxane coincided with that on the PI block, therefore, it is not possible to distinguish between the two on the spectra. Although the role of diphenylsiloxane in the hybrid copolymer awaits to be cleared, it is discussed in detail in another report[36] and data in this respect will not be included in this study. However, we did experience the benefits that came from the addition of diphenylsiloxane.

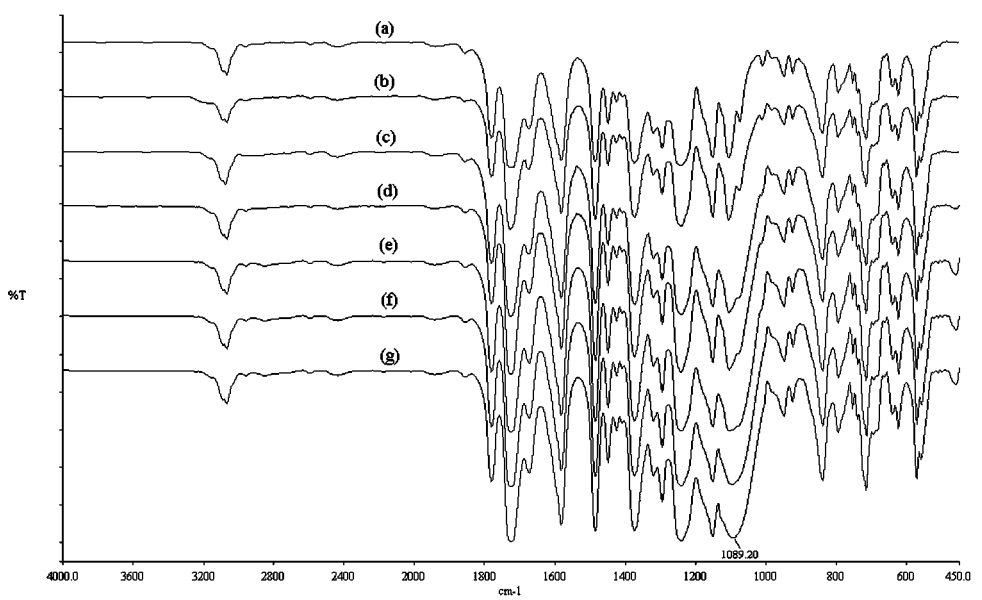

Figure 2 FTIR spectra of PIS/SiO_2 hybrid nanocomposites (a) PIS/SiO_2-1, (b) PIS/SiO_2-7, (c) PIS/SiO_2-12, (d) PIS/SiO_2-15, (e) PIS/SiO_2-20, (f) PIS/SiO_2-25, (g) PIS/SiO_2-30.

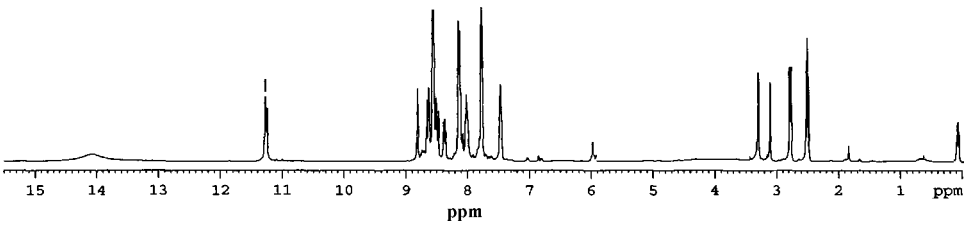

Figure 3 ^{1}H-NMR spectra of the PAAVS.

^{1}H-NMR analysis

Chemical shifts of atoms in NMR spectra can provide insight to molecular structures of organic compounds. We turned to ^{1}H-spectra for more information about the PIS/SiO_2 hybrid nanocomposites. ^{1}H-NMR studies was conducted by dissolving the soluble PIS/SiO_2 hybrid nanocomposite in deuterated dimethylsulfoxide (DMSO-d_6). Figures 3 and 4 represents the ^{1}H-NMR spectra of PAAVS and soluble PIS/SiO_2 hybrid nanocomposites, respectively. The aromatic protons of the BTDA, *m*-BAPS, and diphenylsiloxane gave rise to the signals at δ 7–9 ppm. The signals of the three methylene groups of the terminal amino propyl, of the polysiloxane segment, could be located at δ 0.5, δ 1.8, and δ 2.5 ppm, while the signal near 0 ppm came from the methyl groups of the polydimethylsiloxane *per se*.

The signals of the COOH- and C=C groups, at δ 11.2 and δ 5.9 ppm, are worth noticing here, in that they disappeared when comparing Figures 3 and 4, which indicated that these groups were involved in at least two types of chemical reactions (free-radical reaction, sol-gel reaction, and thermal imidization) during the conversion from PAAVS to PIS/SiO_2 hybrid nanocomposite.

^{29}Si-NMR analysis

Sol-gel reaction is the most important step in the incorporation of inorganic SiO_2 into the hybrid polymer matrix. ^{29}Si-NMR spectra allowed us to monitor the degree of condensation reactions involved in the conversion of Si—OH to Si—O—Si, the two types of Si—O bonding in the final SiO_2 filler. Possible destinies of TEOS and TMVS, used in the sol-gel reaction, were the formation of mono-, di-, tri-, or tetra-substituted siloxane bonds (designated as Q_1, Q_2, Q_3, and Q_4 for TEOS, and T_1, T_2, and T_3 for TMVS). The ^{29}Si-NMR spectra was shown in Figure 5, in which the chemical shifts of Q_2, Q_3, and Q_4 were located at −91, −101, and −109 ppm, respectively. Chemical shifts of T_2 and T_3 can be observed at −69 and −78 ppm, respectively.[37] Comparing relative peak areas corresponding to Q_4 and T_3 showed that they are the major network SiO_2 structure in the hybrid nanocomposite films, whereas Q_4 seemed to be more important, in terms of relative quantity, than T_3.

XRD analysis

XRD was used to determine if the incorporated SiO_2 domain existed, in the PIS/SiO_2 hybrid nanocomposite, as distinct crystal regions or well dispersed SiO_2 particles. Crystalline SiO_2 would give rise to a sharp peak on XRD spectra.[38] Figure 6 showed the XRD spectra of the PIS/SiO_2 hybrid nanocomposites with various SiO_2 content. Broadened peaks at 5–10° and 19–21° indicated that the SiO_2 particles were well dispersed into the PIS matrix.

EDS analysis

EDS spectra was used for elemental analysis for the PIS/SiO_2 hybrid nanocomposite and the spectra was shown in Figure 7. Elemental contents of Si, O, and C were 27, 52, and 21%, respectively. This result confirmed the success of incorporating SiO_2 into the PIS matrix.

Microstructure

SEM can be used to obtain detailed information of the microstructure of the composite material, such as particle sizes and their distributions, at the nanometer level. The SEM micrographs of the cross sections of the PIS/SiO_2 hybrid nanocomposites were shown in Figure 8(a–f). When SiO_2 content was less than

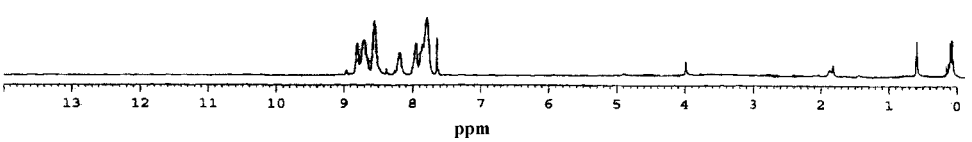

Figure 4 ^{1}H-NMR spectra of the soluble PIS/SiO_2 hybrid nanocomposite.

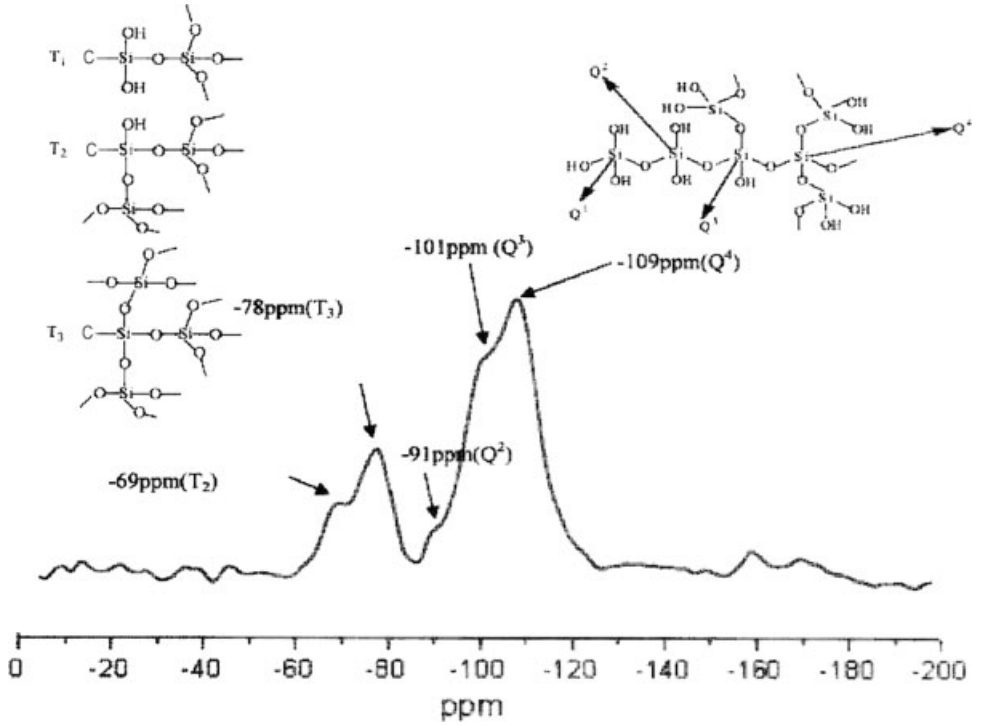

Figure 5 ^{29}Si-NMR spectra of the PIS/SiO_2 hybrid nanocomposite.

10 wt %, the particle size of SiO_2 was smaller than 60 nm. At this nanocomposite level, the film is visually transparent as shown in Table I. Above the level of 10 wt % of SiO_2 content, the particle size increased from 100 nm, at 12 wt %, to 2000 nm at 30 wt % (data of 30 wt % not shown), and the films were opaque.

All micrographs revealed that SiO_2 domains were smooth and bonded with the surrounding PIS matrix, which suggested that there existed strong interfacial adhesion between the two phases. When SiO_2 content was reduced to 7 wt %, the SiO_2 particles were barely distinguishable under SEM (Fig. 8), we had to turn to TEM. Figure 9(a,b) showed that, under TEM, at 7 wt %, the particle size was 30 nm, which reduced to 15 nm at 1 wt % of SiO_2 content.

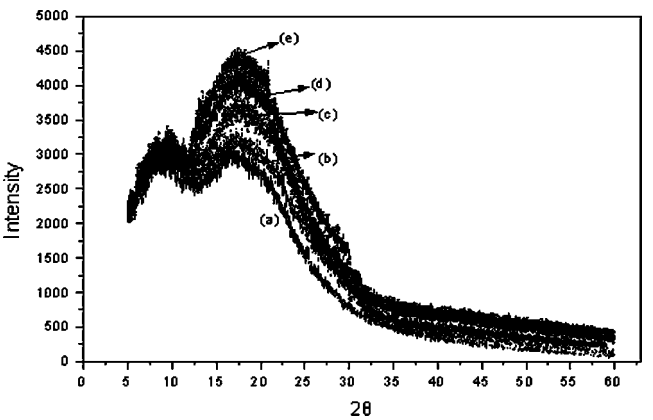

Figure 6 X-ray diffractions for PIS/SiO_2 hybrid nanocomposites (a) PIS, (b) PIS/SiO_2-5, (c) PIS/SiO_2-12, (d)PIS/SiO_2-20, (e) PIS/SiO_2-30.

Thermal properties

When designing new materials, it is important to understand their thermal properties before exploring their potential applications is possible. The T_d and T_g were studied by TGA and DSC, respectively.

Thermal decomposition temperature (T_d)

T_d provides information about the temperature range in which the material of interest is stable. Figure 10

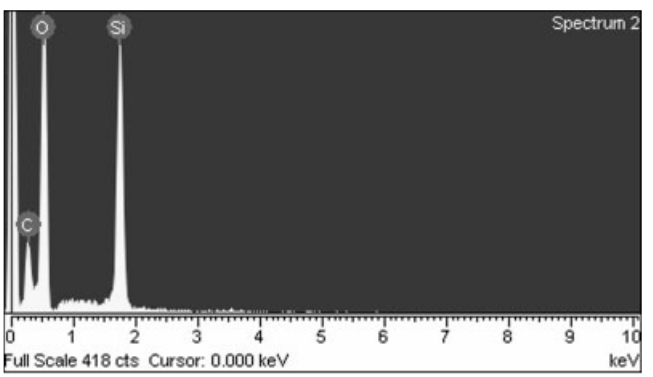

Figure 7 EDS spectra of the PIS/SiO_2-5 hybrid nanocomposite.

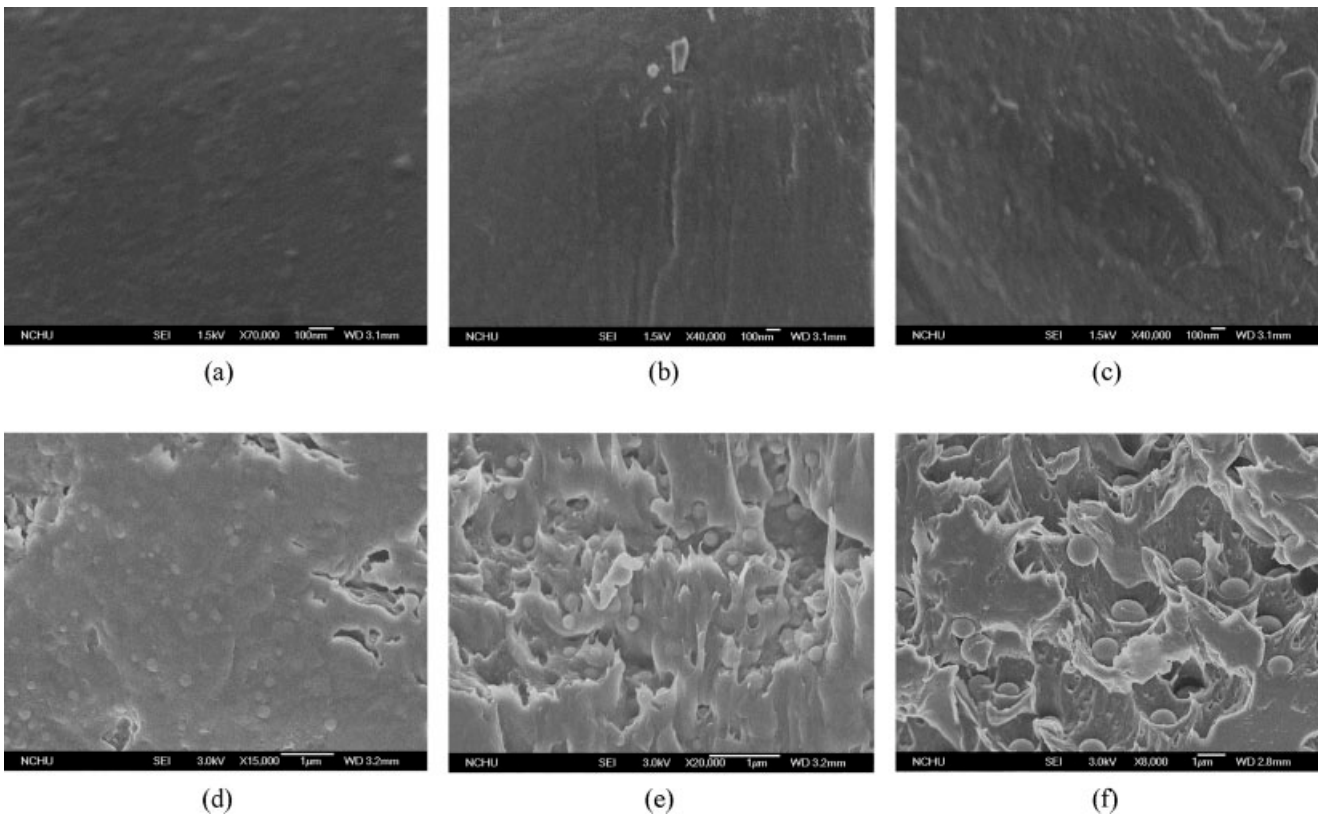

Figure 8 SEM micrographs of the cross section of PIS/SiO_2 hybrid nanocomposites (a) PIS/SiO_2-1, (b) PIS/SiO_2-5, (c) PIS/SiO_2-7, (d) PIS/SiO_2-10, (e) PIS/SiO_2-12, (f) PIS/SiO_2-15.

depicted the TGA curves of the PIS/SiO_2 hybrid nanocomposite at various SiO_2 content. No weight loss was observed at temperature below 100°C, indicating that there was no residual water or ethanol. The temperatures at which 5% weight loss occurred were taken as T_d, and were listed in Table II. T_d of PIS copolymer was 531°C, which increased to 535°C after the incorporation of 1 wt % of SiO_2. The

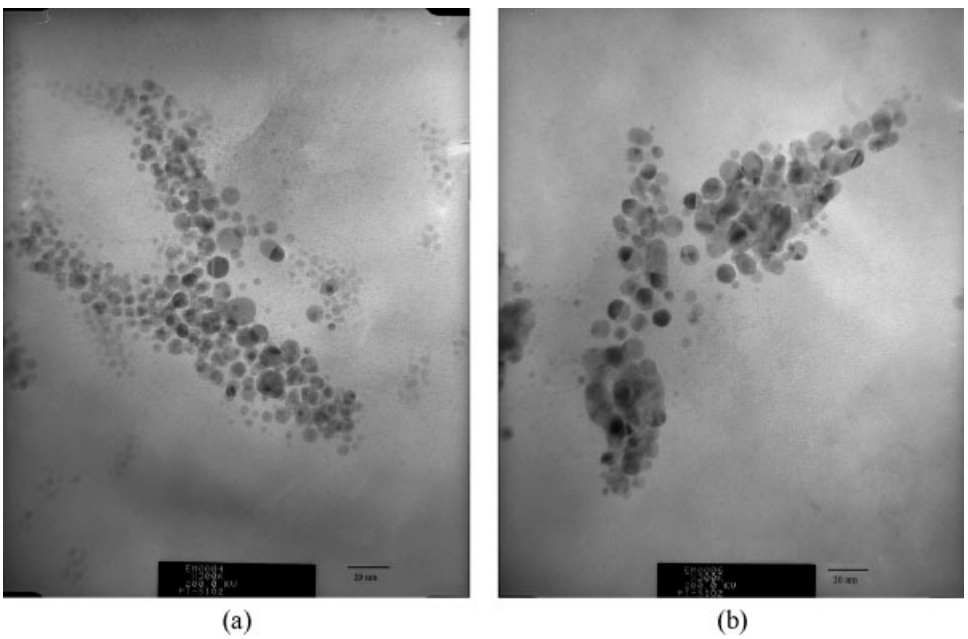

Figure 9 TEM micrographs of PIS/SiO_2 hybrid nanocomposites (a) PIS/SiO_2-1 (b) PIS/SiO_2-7.

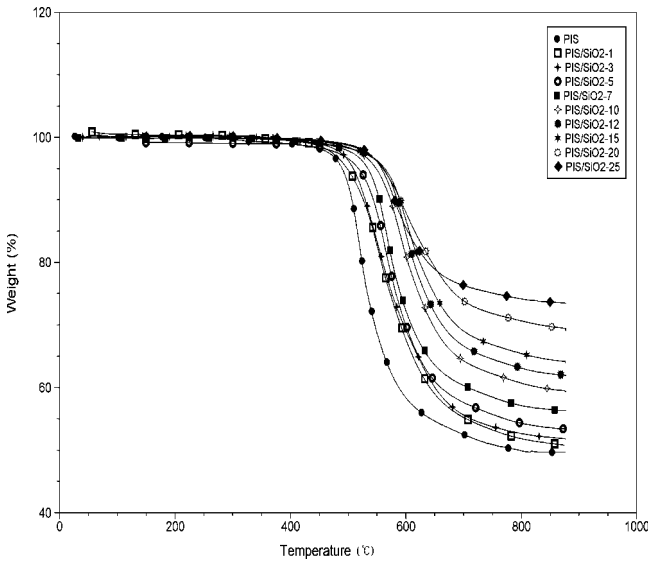

Figure 10 TGA curves of PIS/SiO_2 hybrid nanocomposites of various SiO_2 content.

general trend was that T_d increased with increasing SiO_2 content, until 563°C at SiO_2 content of 15 wt % (Fig. 10). T_d started to decline upon further increase of SiO_2 content.

Glass transition temperature (T_g)

T_g may characterize the upper temperature limit of retaining the sufficient hardness of the material. T_g of the PIS/SiO_2 hybrid nanocomposites at various SiO_2 content were plotted in Figure 11 and were listed in Table II. T_g of PIS copolymer, without the incorporation of SiO_2, was 232.8°C. Figure 11 showed that with the incorporation of SiO_2, T_g increased with increasing SiO_2 content to 242.7°C at 12 wt % SiO_2 content. However, quite similar to that of the T_d study, this trend was reversed when SiO_2 content was higher than 12 wt %.

Considering numerous hydroxyl groups on silicon atom at the surface of the SiO_2 domain, which provided plenty of opportunities in forming hydrogen bonding with the carbonyl groups of the PI matrix, it was not surprising that the introduction of SiO_2 increased the thermal stability. Meanwhile, the dispersed SiO_2 domain, as can be observed in the SEM micrograph, in the continuous PIS phase, offered chances of covalent bonding between the PIS matrix and the SiO_2 network, because of the presence of vinyl groups (on both siloxane and TMVS moieties) before they are crosslinked. At high temperatures, in terms of contribution to thermal stability, covalent bonding may be more important than physical interactions. Albeit important, hydrogen bonding or covalent bonding, large interfacial surface areas (between the SiO_2 domain and the continuous PIS phase) came in even more fundamental, in that they were the basic factor that are responsible for providing vacancies for the formation of either kind of bonding.

In this study, when incorporated SiO_2 was less than 12 wt %, the particle size was smaller than 100 nm, which resulted in a transparent composite film and improved thermal properties. However, studies of either opacity or thermal property, of the composite film, unanimously pointed out that SiO_2 content has a critical value, corresponding to a critical particle size, beyond which, the trend of increased thermal stability with increasing SiO_2 content changed, and meanwhile, the film became opaque.

Turning to SEM and TEM micrographs, this critical value of 12 wt % SiO_2 content corresponded to a particle size of 100 nm. Dispersed SiO_2 nanoparticles

TABLE II
Thermal and Mechanical Properties of the PIS/SiO_2 Hybrid Nanocomposites

Sample name	T_d[a] (°C)	Tg[b] (°C)	Young's modulus[c] (MPa)	Ultimate tensile strength[d] (MPa)	Elongation[e] (%)
PIS	531	232.8	1210	92.8	24.9
PIS/SiO_2-1	535	235.3	1620	94.6	21.9
PIS/SiO_2-3	541	237.1	2130	98.3	16.5
PIS/SiO_2-5	546	239.5	2480	102.6	15.6
PIS/SiO_2-7	550	241.8	3290	104.8	13.2
PIS/SiO_2-10	557	242.2	3598	106.9	10.6
PIS/SiO_2-12	561	242.7	4214	109.3	9.9
PIS/SiO_2-15	563	241.4	4792	114.1	9.8
PIS/SiO_2-20	560	240.5	5257	116.4	8.6
PIS/SiO_2-25	557	240.3	5892	120.1	7.4
PIS/SiO_2-30	553	236.7	6320	122.9	4.5

[a] 5% weight loss temperature (°C) observed in TGA.
[b] Glass transition temperature (°C).
[c] Initial slope of the stress-strain curve.
[d] Stress at break (MPa).
[e] Elongation at break (%).

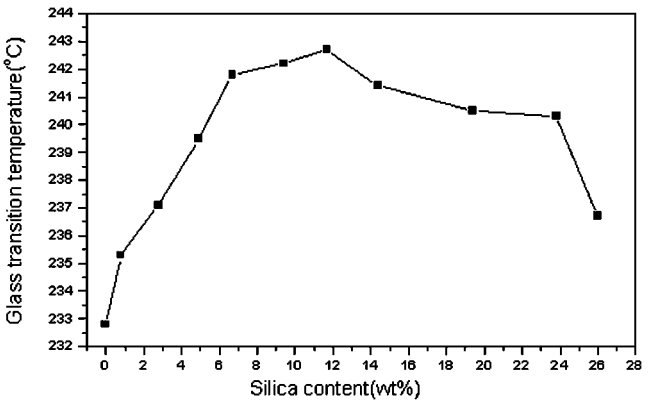

Figure 11 Effect of SiO_2 content on the T_g of the PIS/SiO_2 hybrid nanocomposites.

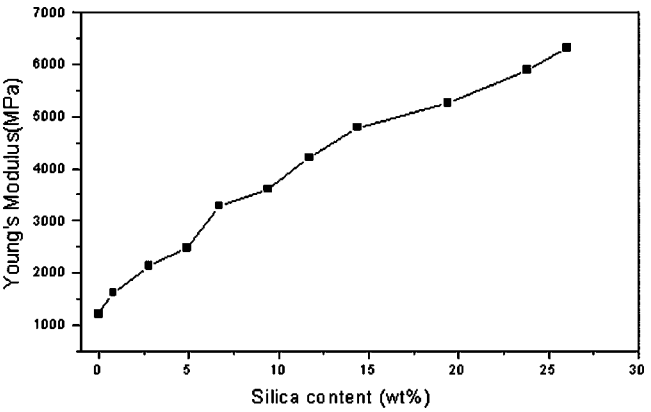

Figure 12 Plot of Young's modulus (MPa) of the hybrid film systems of various SiO_2 content (wt %).

that offered huge interfacial surface area for bond formation might be the main reason for the observed critical point. The SiO_2 nanoparticles played an important role of serving as the physical, as well as chemical crosslinking points, which limited the movement of the molecular chain of PIS and rendered improved thermal properties to the PIS/SiO_2 hybrid nanocomposite. As SiO_2 content was higher than 12 wt %, however, the decline of T_d and T_g could be attributed to increased particle size, which led to a decrease in specific interfacial surface area.

Mechanical properties

The intention of incorporating inorganic SiO_2 into the organic polymer, either physically or chemically (covalent bond formation), was mainly for the purpose of improving mechanical properties. In this study, SiO_2 served this purpose positively to different extent, depending on SiO_2 content, as listed in Table II. In general, the ultimate strength and Young's modulus increased with increasing SiO_2 content, while SiO_2 content affected the ultimate elongation conversely.

Young's modulus

Figure 12 depicted the relationship between the Young's modulus and the SiO_2 content. The Young's modulus increased approximately linearly with SiO_2 content for most of the range studied. However, the trend slightly curved upward when SiO_2 content was higher than 20 wt %, and resulted in an impressively high Young's modulus of 6320 MPa at SiO_2 content of 30 wt %.

Ultimate tensile strength and elongation at break

The ultimate tensile strength and elongation at break of the PIS/SiO_2 hybrid nanocomposite were plotted against SiO_2 content in Figure 13. Without the incorporation of SiO_2, the PIS copolymer film possessed an ultimate tensile strength of 92.8 MPa, which is already a remarkable value. However, it would be interesting to see if the incorporation of inorganic SiO_2 could further improve the mechanical property in this respect.

At SiO_2 content of 1 wt %, the ultimate tensile strength increased to 94.6 MPa and steadily increased to 122.9 MPa at 26 wt %. This phenomenon could be attributed to both the strong physical interactions between organic and inorganic phases, and the chemical bond between the siloxane segment of PIS and the SiO_2 particles.

Chen[28] and Ahmad[17] also studied the PI/SiO_2 hybrid material in which chemical bond formation between PI and the SiO_2 network was developed. The hybrid films were prepared by hydrolysis and polycondensation of aminopropyltriethoxysilane, the terminal group of PI and TEOS in the polymer solution in N, N′-dimethylacetamide (DMAc). They

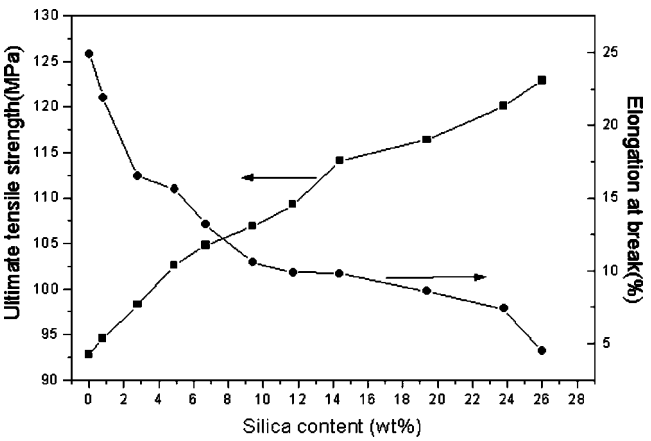

Figure 13 Plot of ultimate tensile strength (MPa) and elongation at break (%) of the hybrid film systems of various SiO_2 content.

found in comparison to the PI, samples containing SiO_2 have higher ultimate tensile strength and higher modulus, but lower elongation. Thus, it was proposed that the ultimate properties of the hybrids depend on the extent of bond formation between the two phases.

Elongation at break is an important mechanical property for materials of this category. The presence of polysiloxane segment rendered the PIS copolymer improved flexibility and the elongation at break was as high as 24.9%. The incorporation of SiO_2 tends to counteract the contribution of polysiloxane and reduced the elongation at break (Fig. 13). However, the effect of decreasing the elongation at break was less significant at SiO_2 content higher than 2.8 wt % (PIS/SiO_2-3). Although it remains to be seen, should counterbalancing the SiO_2 effect on increased hardness be desirable, the amount of polysiloxane added may be an important parameter in the engineering of the hybrid nanocomposites.

CONCLUSIONS

The organic PIS copolymer, with the aid of TEOS, has been successfully incorporated with inorganic SiO_2 which forms a SiO_2 network with C-Si covalent bondings at the interface. Microstructure of well dispersed nano-sized SiO_2 particles rendered special properties to this new hybrid nanocomposite, such as optical transparency and improved mechanical as well as thermal properties. SiO_2 content played a key role in affecting important features of the hybrid nanocomposites, and could be a parameter to be manipulated in designing the new hybrid nanocomposites for various applications.

References

1. Tsujita, Y.; Yoshimura, K.; Yoshimizu, H.; Takizawa, A.; Kinoshita, T. Polymer 1993, 34, 2597.
2. Sacher, E.; Schreiber, H. P.; Wertheimer, M. R. J Appl Polym Sci: Appl Polym Symp 1984, 38, 163.
3. Ying, L.; Edelman. 31st National Sample Symposium 1986, 31, 1131.
4. Thompson, L. F.; Willos, C. G.; Tagawa, S. E. Polymers for Microelectronics: Resiets and Dielectrics; American Chemical Society: Washington, DC, 1994; p 380.
5. Policastro, P. P.; Lupinski, J. H.; Hernandez, P. K. Polymeric Materials for Electronics Packaging and Interconnection; American Chemical Society: Washington, DC, 1989; p 140.
6. Tamai, S.; Yamaguchi, A.; Ohta, M. Polymer 1996, 37, 3683.
7. Goizet, S.; Schrotter, J. C.; Smaihi, M.; Deratani, A. New J Chem 1997, 21, 461.
8. Chang C. C.; Chen, W. C. J Polym Sci Part A: Polym Chem 2001, 39, 3419.
9. Joly, C.; Smaihi, M.; Porcar, L.; Noble, R. D. Chem Mater 1999, 11, 2331.
10. Sysel, P.; Hobzova, R.; Sindelar, V.; Brus, J. Polymer 2001, 42, 10079.
11. Huang, Y.; Gu, Y. J Appl Polym Sci 2003, 88, 2210.
12. Ha, C. S.; Cho, W. J Polym Adv Technol 2000, 11, 145.
13. Huang, J. C.; Zhu, Z. K.; Yin, J.; Zhang, D. M. J Appl Polym Sci 2001, 79, 794.
14. Ha, C. S.; Park, H. D.; Frank, C. W. Chem Mater 2000, 12, 839.
15. Nandi, M.; Conklin, J. A.; Salvati, L.; Sen, A. Chem Mater 1991, 3, 201.
16. Morilawa, A.; Iyoku, Y.; Kakimoto, M.; Imai, Y. Polym J 1992, 24, 107.
17. Ahmad, Z.; Mark, J. E. Chem Mater 2001, 13, 3320.
18. Maryska, M.; Sysel, P.; Pulec, R. Polym J 1997, 29, 607.
19. Hsiue, G. H.; Chen, J. K.; Liu, Y. L. J Appl Polym Sci 2000, 76, 1609.
20. Chris, J.; Cornelius, E. M. Polymer 2002, 43, 2385.
21. Bershtein, V. A.; Egorova, L. M.; Yakushev, P. N.; Pissis, P.; Sysel, P.; Broxova, L. J Polym Sci Part B: Polym Phys 2002, 40, 1056.
22. Kandary, A. S.; Ali, M. A. A.; Ahmad, Z. J Appl Polym Sci 2005, 98, 2521.
23. Chang, C.; Wei, K.; Chang, Y.; Chen, W. J Polym Res 2003, 10, 1.
24. Park, Y. W.; Lee, D. S. J Appl Polym Sci 2004, 93, 342.
25. Wang, S.; Ahmad, Z.; Mark, J. E. Chem Mater 1994, 6, 943.
26. Schrotter, J. C.; Smaihi, M.; Guizard, C. J. J Appl Polym Sci 1996, 61, 2137.
27. Sysel, P.; Pulec, R.; Maryska, M.; Polym J 1997, 29, 607.
28. Chen, J.; Iroh, J. O. Chem Mater 1999, 11, 1218.
29. Shang, X. Y.; Shu, Z. K.; Yin, J.; Ma, X. D. Chem Mater 2002, 14, 71.
30. Chen, B. K.; Chiu, T. M.; Tsay, S. Y. J Appl Polym Sci 2004, 94, 382.
31. Landry, C. T.; Coltrain, B. K.; Teegarden, D. M.; Long, T. E.; Lomg, V. K. Macromolecular 1996, 29, 4712.
32. Park, H. B.; Kim, J. H.; Kim, J.; Lee, Y. M. Macromol Rapid Commun 2002, 23, 544.
33. Takekoshi, T. In Polyimides: Fundamentals and Applications; Ghosh, M. K.; Mittal, K. L., Eds.; Marcel Dekker: New York, 1996; Chapter 2.
34. Morikawa, A.; Iyoku, Y.; Kakimoto, M.; Imai, Y. Polym J 1992, 24, 107.
35. Srinivasan, S. A.; Hedrick, J. L.; Miller, R. D. Polymer 1997, 38, 3129.
36. Liaw, W. C.; Chen, K. P. J Polym Res 2007, 14, 5.
37. Chiang, C. L.; Ma, M. C. H.; Wu, D. L.; Kuan, H. C. J Polym Sci Part A: Polym Chem 1999, 37, 2275.
38. Lu, C.; Wang, Z.; Liu, F.; Yan, J.; Gao, L. J Appl Polym Sci 2006, 100, 124.